In situ resonant UV-raman spectroscopy of polycyclic aromatic hydrocarbons

In situ Resonant UV-Raman Spectroscopy of Polycyclic Aromatic Hydrocarbons

Matteo Signorile[†], Francesca Bonino[†]*, Alessandro Damin[†], and Silvia Bordiga[†]

[†] Department of Chemistry, NIS and INSTM Reference Centre, University of Turin, Via G. Quarello 15, I-10135 and Via P. Giuria 7, I-10125, Turin, Italy

* Francesca Bonino, Tel: +39-011-6708383, Fax: +39-011-6707855, E-mail: francesca.bonino@unito.it

Keywords

Raman spectroscopy - Polycyclic Aromatic Hydrocarbons - Heterogeneous catalysis – Coke - Zeolites

Abstract

PAHs are hazardous and persistent pollutants, also found as byproducts of some petrolchemical reaction (e.g. MTH) in relation to the catalyst deactivation, i.e. to the formation of coke species. The analysis of such deactivation products is typically performed by means of chromatographic techniques, with some drawbacks: the extraction and separation of the molecules from the matrix (the catalyst) is always required and the solubility of the larger ones is often very low also in non-polar solvents, so that their analysis is not possible with a standard approach.

Spectroscopies can represent an interesting alternative for the qualitative analysis of PAHs: in particular Raman spectroscopy has been demonstrated to be a powerful tool in the

characterization of carbonaceous materials and PAHs and the possibility to exploit the resonance effect (allowing the selective enhancement of vibrational features of the resonant species) can be a considerable advantage in the analysis of very diluted species. In the present work, PAHs have been characterized by means of UV Raman spectroscopy: the 244 nm excitation wavelength allowed to exploit the resonance effect and in the meantime to avoid interference due to the visible fluorescence typical of these molecules. A pool of representative PAHs have been analyzed in their pure form, in diluted solution and dispersed on high surface area microporous supports: the collected data constitute a reference database to be compared with the deactivation products observed during petrolchemical reactions, offering the possibility to univocally identify them.

Introduction

Polycyclic aromatic hydrocarbons (PAHs) are a class of molecules with relevance in several scientific fields. Originating from the incomplete combustion of organic matter at high temperature, both from natural (wood fires,[1] geothermal activity[2]) and anthropogenic (combustion of fossil fuels[3]) activities, PAHs are dangerous pollutant because of their mutagenic/carcinogenic activity[4,5] and their environmental persistence related to their relatively low hydrophilicity.[6] PAHs are also found as ubiquitous components of the interstellar medium and their study is relevant in the understanding several astrophysical and astrochemical processes.[7,8] In the field of heterogeneous catalysis, PAHs originate as byproducts of petrolchemical processes: a significant example is represented by the methanol to hydrocarbons (MTH) reaction, where the formation of large aromatic molecules (i.e. coke precursors) inside the channels/cages of the zeolite based catalyst leads to a progressive reduction of the catalytic

activity (i.e. to the catalyst deactivation).[9-11] These molecules, unable to diffuse out of the cavities, make the active sites hindered to the reactants reducing the overall catalyst activity. The detection of such molecules is typically performed through chromatographic methods:[12,13] in the specific case of the characterization of coke residuals in zeolites, a widely applied analytical methodology involves the dissolution of the siliceous framework in hydrofluoric acid is followed by GC/MS analysis of the dichloromethane soluble residuals.[9,10] The main drawback related to this procedure is the impossibility to analyze the heavier fraction of coke, which is not soluble in the most common solvents and whose components have a too high molecular weight to be analyzed by standard GC/MS.

A possible alternative tool for the characterization of such molecules can be represented by Raman spectroscopy, which finds large application in the study of carbonaceous materials.[14-16] Each PAH shows a peculiar vibrational spectrum, allowing to determine the nature of the coke species. The main drawback related to the application of Raman is the possible fluorescence of the sample: PAHs are highly emissive in the visible region and their fluorescence bands can overlap the Raman signal. Generally such interference can be avoided by using an excitation wavelength falling outside of the visible range (i.e. IR or UV excitation lasers).[17] In this regard, some pioneering studies demonstrated the relevance of UV Raman spectroscopy in the characterization of spent (i.e. coked) zeolite catalysts.[18-22] A further advantage related to the UV Raman characterization of PAHs is due to the electronic transitions of such molecules, falling in the 200-400 nm spectral region:[23-25] this allows to exploit the resonance conditions, i.e. to increase of orders of magnitude the sensitivity of Raman spectroscopy toward PAHs, significantly reducing their limit of detection and allowing their analysis even diluted.[26] Being in a real catalytic system the coke species dispersed on a porous material with high surface area, the

possibility to exploit the resonance makes feasible their characterization, even *in situ*. Beside the resonance, the probable photochemical damage of the sample promoted by an intense UV radiation, especially dealing with organic adsorbates,[19,22] has to be avoided. A specifically designed home-made sample holder was adopted in this regard. In the present study a pool of representative PAHs (whose structures are reported in **Figure 1**) has been selected and characterized by off-resonance visible Raman and resonance UV Raman spectroscopy, collecting an unique spectroscopic database that represent a first step toward the in situ and in operando characterization of coke species when highly diluted in the reaction environment.

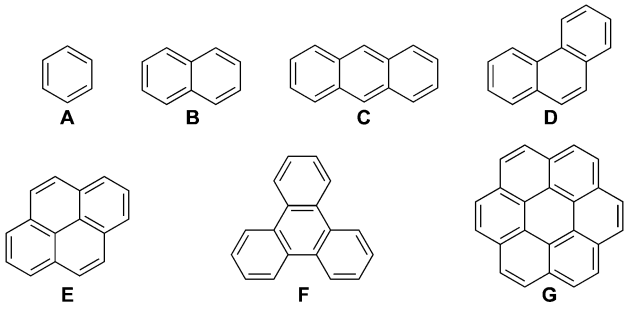

Figure 1. Structures of benzene **A**; naphthalene **B**; anthracene **C**; phenanthrene **D**; pyrene E; triphenylene **F**; and coronene **G**.

Experimental

Seven representative aromatic molecules have been selected for this study: benzene (Fluka, ≥99.5%); naphthalene (Fluka, ≥99%); phenanthrene (Aldrich, ≥97%); anthracene (Fluka, ≥99%); pyrene (Aldrich, ≥98%); triphenylene (Aldrich, ≥98%); and coronene (Aldrich, ≥97%).

The Raman and resonant UV Raman characterization of such molecules has been performed in three different conditions: i) on the pure molecules; ii) on the same set of molecules diluted in acetonitrile (Aldrich, UV grade ≥99.9%), hereafter ACN); iii) or dosed from their vapor phases

onto Aerosil 300 (Evonik, 300 m^2g^{-1}), Silicalite-1 (hereafter S-1, home made according to Guth et al. [27], 550 m^2g^{-1}) and coconut origin granular carbon (Chimet, 1400 m^2g^{-1}).

All the solid supports have been activated before dosing the molecules in order to remove all the previously adsorbed species. Silicalite-1 and Aerosil 300 have been pelletized and then thermally treated: after 1 hour of outgassing at 500°C, 100 mbar of O_2 (equilibrium pressure inside the cell) have been dosed and left in contact for 1 hour. A monolith of activated carbon has been used instead than a pellet. The activation has been performed outgassing the sample for 1 hour at 150°C. The vapor pressure of each molecule has been dosed on the supports after the activation.

The characterization has been performed by mean of visible and UV Raman spectroscopy. The visible Raman spectra have been collected on a Renishaw inVia Raman Microscope spectrometer, working in backscattering mode equipped with two different excitation laser lines: an Ar^+ laser emitting at 514.5 nm and a Renishaw diode laser emitting at 785nm. The UV Raman characterization has been performed with a Renishaw Raman System 1000, provided with a frequency doubled Ar^+ laser operating at 244 nm. Particular effort has been done to avoid sample photochemical damage, adopting a specifically designed home-made sample holder. Figure S1 in the Supporting Information reports a clear case in which the sample undergoes to photochemical decomposition.

The collected Raman spectra are characterized by very different intensities due to the different extent of the resonance of the analyzed molecules. In order to improve the comparison of the spectra, a normalization in the intensity range between 0 and 1 has been applied. Furthermore the normalized spectra have been shifted along the intensity axis for sake of visualization.

Results and Discussion

The visible (λ = 785 nm and 514 nm) and UV (λ = 244 nm) Raman spectra of the molecules as such are reported in Figure 2.

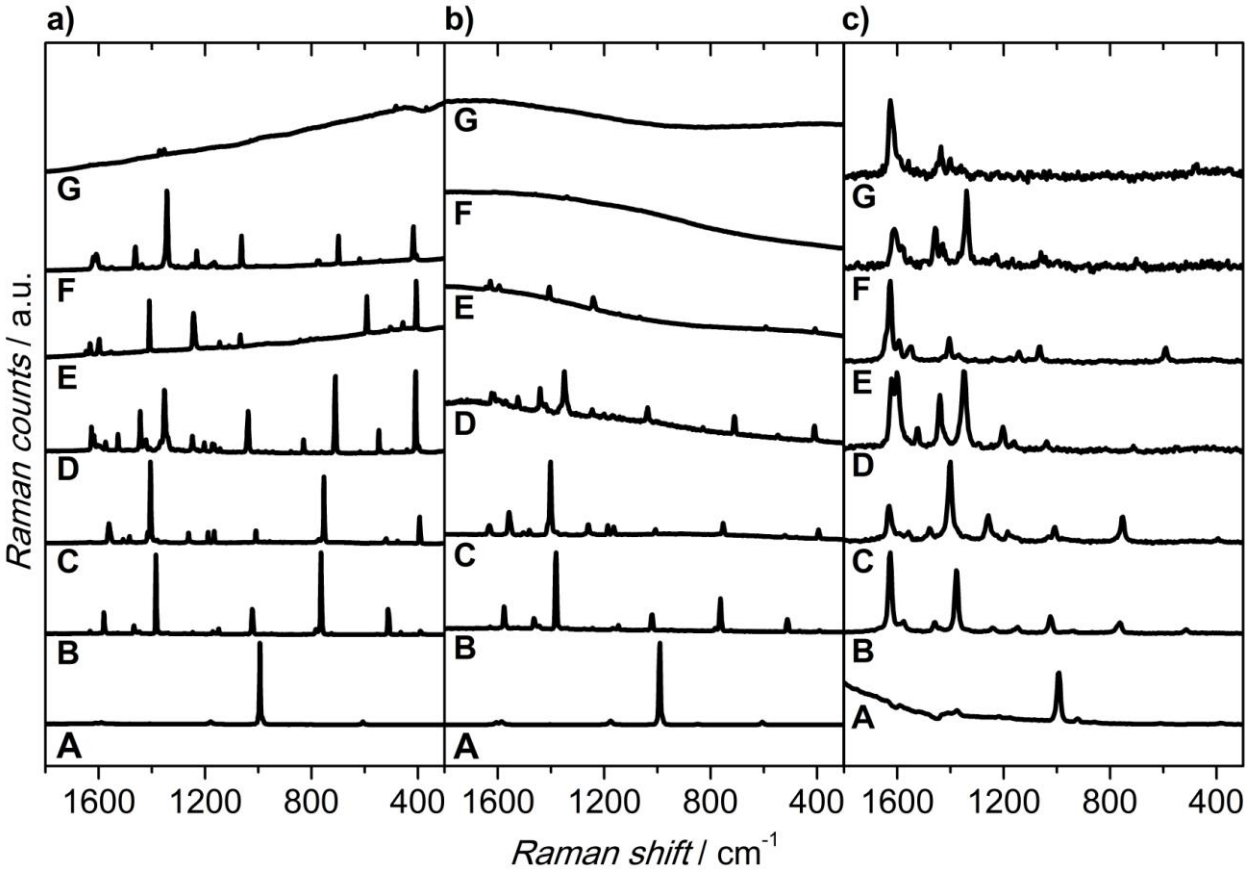

Figure 2. Raman spectra obtained by means of three different exciting laser lines: part a) λ = 785 nm; part b) λ = 514 nm and part c) λ =244 nm respectively of: benzene **A**, naphthalene **B**, anthracene **C**, phenanthrene **D**, pyrene **E**, triphenylene **F** and coronene **G**. Spectra have been rescaled and shifted for a better comparison.

While UV Raman spectra can be obtained without relevant interferences in any case, the visible Raman spectra of coronene (curve G, Figure 2a andFigure **2**b) and triphenylene (curve F, Figure 2b) are dominated by their fluorescence profiles. Such problem is well known,[26] as well as the advantage of the use of the UV excitation wavelength due to the electronic transitions of most of the investigated molecules falling across the near-UV and the first visible (as

demonstrated in Figure S2).[23,24] In fact UV Raman spectra show different relative intensities in comparison with those ones obtained with a visible laser line.

The typical vibrational modes of PAHs are observed approximately in the 1600-1350 cm^{-1} region: the modes falling around 1600 cm^{-1} are roughly comparable to the G band observed in the graphitic materials, due to in-plane bond stretching motion of C sp^2 atoms pairs. Instead the vibrations around 1350 cm^{-1} show similarities to the collective breathing modes of the hexagonal rings, generally labeled as D band.[14,28] Some of these vibrations are selectively enhanced by using the UV excitation source thanks to the Raman resonance. It is worth to underline the full understanding on the origin of the resonance implies to consider the contribution of more complex effects (such as the Herzberg-Teller) causing the enhancement of low symmetry vibrational modes as well. An accurate description of this kind of mechanism in PAHs has been recently given by Avila Ferrer and coworkers on the basis of advanced ab initio simulations.[29]

The possibility to exploit the resonance with a considerable improvement in the spectra quality in terms of signal to noise ratio allowed us to move toward the study of PAHs diluted in different matrices. As the simplest approach we focused on the characterization of the molecules dissolved in ACN. The obtained spectra are reported in **Figure 3**. The determining role of resonance is clearly depicted by this series of spectra: when the resonance conditions are achieved, the signal of the solvent is almost nil (even without subtracting the contribution of solvent from the raw spectra) and all the most intense peaks are exclusively related to the analyte (while the off-resonance visible Raman is never sufficiently sensitive to detect the solutes, as exemplified in Figure S3 of the Supporting Information). Nevertheless, molecules such as coronene and benzene are hardly detectable even by UV Raman. In the case of coronene, its electronic transitions fall quite far below the excitation laser frequency,[30] so that the resonance conditions

are not achieved and the spectrum is dominated by the vibrational fingerprints of ACN. The absence of appreciable signals related to the benzene instead is ascribable to more complex phenomena: first of all the excitation frequency falls very close to the $S_0 \rightarrow S_1$ electronic transition of benzene,[24] so that the excitation photons are for the larger part absorbed rather than scattered by the benzene. Furthermore this molecule shows a relevant fluorescence in the investigated spectral region (see Figure S4 of the Supporting Information), which can interfere with the detection of the analyte signals. The combination of these effects can explain the lack of signals ascribable to the benzene and the poor intensity of the vibrational fingerprints of the ACN.

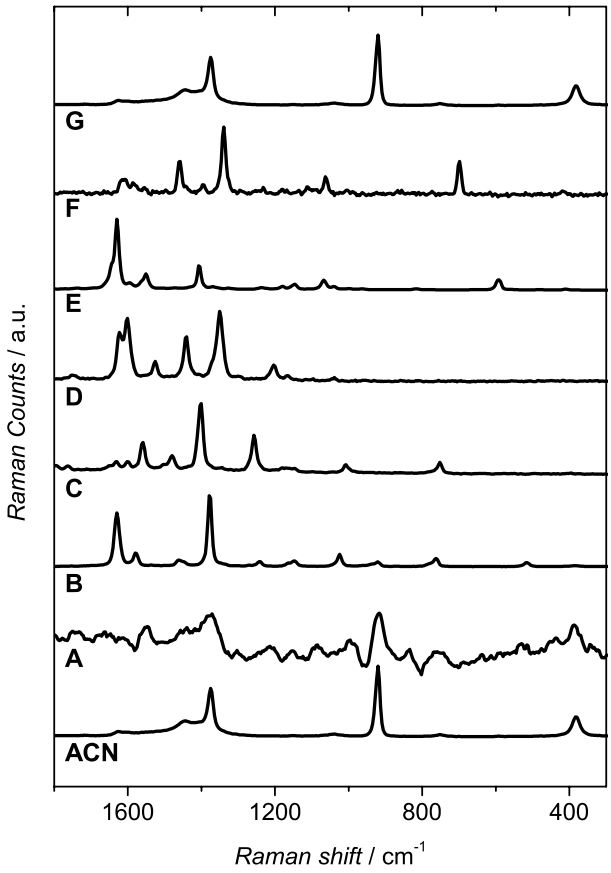

Figure 3. UV (λ = 244nm) Raman spectra of 0.1M solutions in ACN of benzene **A**, naphthalene **B**, anthracene **C**, phenanthrene **D**, pyrene **E**, triphenylene **F** and coronene **G**. Spectra have been rescaled and shifted for a better comparison.

Even if the molecules can be easily observed as diluted species in solution, this kind of situation is substantially far from the real systems where PAHs are highly dispersed on an heterogeneous catalyst (i.e. on complex solid support). In order to produce data comparable with those ones, we moved toward the dispersion of the molecules on some representative model solid supports. Firstly, we measured the PAHs adsorbed from gas phase on Silicalite-1 (S-1) and Aerosil 300 (SiO_2) (see Figure 4a and 4b). Silcalite-1 has been preferred to an acid MFI zeolite (i.e. the real catalyst) as the proton/aromatic molecule interaction can give rise to the formation

of carbocationic species,[31,32] whose investigation is out of the scope of the present work. Aerosil 300 instead has been chosen being a purely siliceous and high surface area material (as S-1 is), but showing a completely different structure (amorphous vs. crystalline) and pore system (inter-particle pores vs. ordered 3D porous channels). The comparison of the Raman spectra of PAHs adsorbed on these materials is useful in order to recognize the possible confinement of the molecules inside the micropores of the zeolite (resulting in a shift of their vibrational modes),[33] as such effect it is not expected in a system with a wider porosity. Secondly, the dosage of PAHs has been performed on an activated carbon (see Figure 4c), with the goal to simulate the heavier coke deposits (i.e. highly defective sp^2 materials) formed inside the real catalyst pores. As the dosage of the molecules depends on their vapor pressure, the collection of the Raman spectra of the heavier molecules (triphenylene and coronene) was not possible, as their concentration in the gas phase was definitely too low in order to allow their detection as adsorbates.

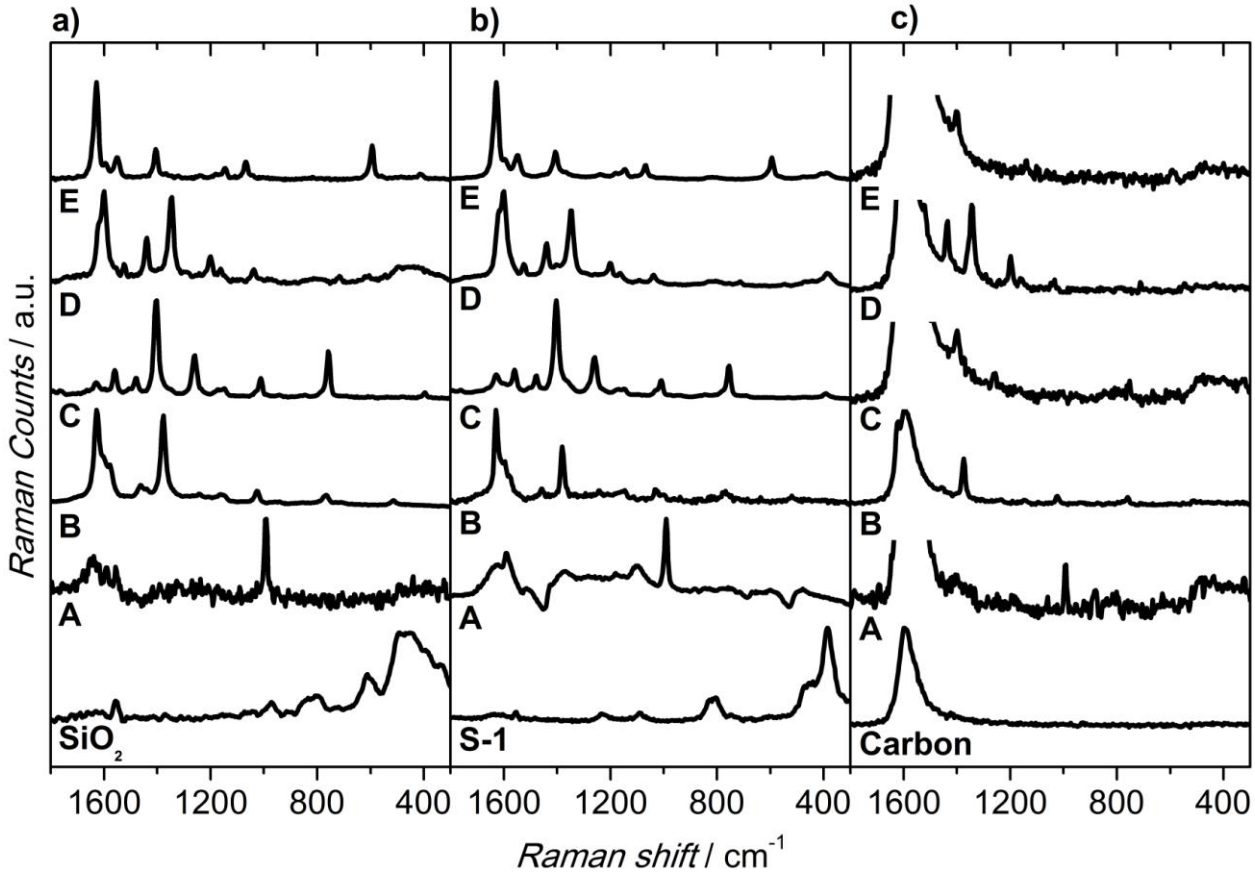

Figure 4. UV (λ=244nm) Raman spectra of benzene **A**, naphthalene **B**, anthracene **C**, phenanthrene **D** and pyrene **E** adsorbed from vapor phase on Silicalite-1 a); Aerosil 300 b); and activated carbon c). The spectra of the adsorption supports spectra are also reported. Spectra have been rescaled and shifted for a better comparison.

Being the resonance achieved, in the case of Silicalte-1 (Figure 4a) and Aerosil 300 (Figure 4b) the signal related to the support is completely negligible in comparison with PAHs ones. The detection of PAHs is possible even on the activated carbon, despite its extremely high optical absorption (Figure 4c). The main limitation of the UV Raman spectroscopy in this last case is the overlapping of the carbon G band (around 1600 cm^{-1}) with the PAHs signal. However the 1000-1400 cm^{-1} frequency region is free from any support interferences, so that the vibrational fingerprints of the analytes can be clearly recognized and assigned. Furthermore, subtracting the

Raman spectrum of the bare activated carbon, the vibrational pattern of the net molecules can be reconstructed (Figure S5 of the Supporting Information). Although, the subtracted spectra are affected by heavy noise, making them not fully reliable in terms of relative intensities.

The main vibrational fingerprints for each molecule (univocally identifying them) are reported in Table 1.

Table 1. Summary of main vibrational fingerprints for each molecule in each analysed state.

	Pure	ACN	S-1	Aerosil	Carbon
Benzene	992	-	991	991	991
Naphtalene	1626	1630	1630	1628	1621
	1379	1379	1380	1377	1374
	1024	1024	1029	1027	1023
Anthracene	1400	1401	1402	1402	1399
	1257	1258	1259	1259	1256
	752	753	755	758	752
Phenanthrene	1601	1601	1600	1600	-
	1440	1439	1439	1439	1434
	1350	1350	1346	1346	1345
Pyrene	1626	1630	1629	1628	-
	1404	1408	1407	1406	1399
	591	591	594	594	590
Triphenylene	1458	1458	-	-	-
	1339	1340	-	-	-
	702	698	-	-	-
Coronene	1626	-	-	-	-
	1436	-	-	-	-
	1400	-	-	-	-

It is interesting to note that the environment slightly affects the vibrational modes of the molecules, but these shifts are sufficiently small to easily allow the recognition of the different moieties in any case. The only relevant difference is encountered when PAHs are dosed on the activated carbon: all the considered vibrational frequencies are significantly red-shifted with

respect to the ones of pure molecules. Such effect is probably related to the higher affinity of carbon toward PAHs (due to their similarities in terms of structure), but it is not easily rationalizable without the support of molecular modeling and its full understanding is out of the aim of this research work.

The confinement effect expected from the microporosity of Silicalite-1 has not been observed as the observed shifts are definitely negligible with respect to the Aerosil 300. Taking in account the low diffusivity and/or the steric hindrance of PAHs (which don't allow their diffusion inside the zeolitic channels) it is possible to infer that the reported data are representative for the molecules adsorbed on the external surfaces of Silicalite-1, i.e. on a siliceous surface very similar to the Aerosil 300 one.

Conclusions

The presented spectra represent an unique dataset for the analysis of PAHs by means of Raman (in particular UV-Raman) spectroscopy. Exploiting the resonance, the molecules have been analyzed in several environment at different dilutions. The possibility to characterize the PAHs as dispersed species on solid porous materials has been proved as well. The UV-Raman spectroscopy can be regarded as a powerful tool in the characterization of the coke like species forming upon deactivation of the zeolite based catalysts, thanks to the superior sensitivity guaranteed by the resonance effect. Furthermore Raman spectroscopy could be exploited in operando conditions, i.e. allowing the coke characterization directly on the catalyst, while, for the most commonly used chromatographic techniques, the extraction of the reaction byproducts is required.

Supporting Information.

The UV Raman spectra of naphtalene collected preventing/not preventing photodecomposition are reported in Figure S1. In Figure S2 the absorption spectra of the 10^{-5} M solutions of PAHs are presented. Figure S3 shows the Raman spectra of 0.1M solution in acetonitrile of naphthalene collected with different excitation laser lines. In Figure S4 the UV Raman spectrum of 0.1M solution of benzene in acetonitrile in the 3100-300 cm^{-1} frequency range is shown. The background subtracted UV Raman spectra of molecules adsorbed from vapor phase on activated carbon are reported in Figure S5. This material is available free of charge via the Internet at http://pubs.acs.org.

Acknowledgment

The authors acknowledge prof. Claudia Barolo for the supply of some of the samples and dr. Riccardo Pellegrini (Chimet S.p.A.) for providing the granular activated carbon. The authors acknowledge Haldor Topsøe A/S for financial support to the project.

References

1. Schauer, J. J.; Kleeman, M. J.; Cass, G. R.; Simoneit, B. R. T. Measurement of Emissions from Air Pollution Sources. 3. C-1-C-29 Organic Compounds from Fireplace Combustion of Wood. *Environ. Sci. Technol.* **2001**, *35*, 1716-1728.

2. Botz, R.; Wehner, H.; Schmitt, W.; Worthington, T. J.; Schmidt, M.; Stoffers, P. Thermogenic Hydrocarbons from the Offshore Calypso Hydrothermal Field, Bay of Plenty, New Zealand. *Chem. Geol.* **2002**, *186*, 235-248.

3. Rogge, W. F.; Hildemann, L. M.; Mazurek, M. A.; Cass, G. R.; Simoneit, B. R. T. Sources of Fine Organic Aerosol .2. Noncatalyst and Catalyst-Equipped Automobiles and Heavy-Duty Diesel Trucks. *Environ. Sci. Technol.* **1993**, *27*, 636-651.

4. *Iarc Monographs on the Evaluation of the Carcinogenic Risk of Chemical to Humans*; IARC: Lyon, 1986; Vol. 38.

5. Goldman, R.; Enewold, L.; Pellizzari, E.; Beach, J. B.; Bowman, E. D.; Krishnan, S. S.; Shields, P. G. Smoking Increases Carcinogenic Polycyclic Aromatic Hydrocarbons in Human Lung Tissue. *Cancer Res.* **2001**, *61*, 6367-6371.

6. Johnsen, A. R.; Wick, L. Y.; Harms, H. Principles of Microbial Pah-Degradation in Soil. *Environ. Pollut.* **2005**, *133*, 71-84.

7. Sandford, S. A., et al. Organics Captured from Comet 81p/Wild 2 by the Stardust Spacecraft. *Science* **2006**, *314*, 1720-1724.

8. Tielens, A., Interstellar Polycyclic Aromatic Hydrocarbon Molecules. In *Annual Review of Astronomy and Astrophysics*, Annual Reviews: Palo Alto, 2008; Vol. 46, pp 289-337.

9. Bjorgen, M.; Svelle, S.; Joensen, F.; Nerlov, J.; Kolboe, S.; Bonino, F.; Palumbo, L.; Bordiga, S.; Olsbye, U. Conversion of Methanol to Hydrocarbons over Zeolite H-Zsm-5: On the Origin of the Olefinic Species. *J. Catal.* **2007**, *249*, 195-207.

10. Teketel, S.; Skistad, W.; Benard, S.; Olsbye, U.; Lillerud, K. P.; Beato, P.; Svelle, S. Shape Selectivity in the Conversion of Methanol to Hydrocarbons: The Catalytic Performance of One-Dimensional 10-Ring Zeolites: Zsm-22, Zsm-23, Zsm-48, and Eu-1. *ACS Catal.* **2011**, *2*, 26-37.

11. Olsbye, U.; Svelle, S.; Bjorgen, M.; Beato, P.; Janssens, T. V. W.; Joensen, F.; Bordiga, S.; Lillerud, K. P. Conversion of Methanol to Hydrocarbons: How Zeolite Cavity and Pore Size Controls Product Selectivity. *Angew. Chem.-Int. Edit.* **2012**, *51*, 5810-5831.

12. Moret, S.; Conte, L. S. Polycyclic Aromatic Hydrocarbons in Edible Fats and Oils: Occurrence and Analytical Methods. *J. Chromatogr. A* **2000**, *882*, 245-253.

13. Schmidt, T. C.; Zwank, L.; Elsner, M.; Berg, M.; Meckenstock, R. U.; Haderlein, S. B. Compound-Specific Stable Isotope Analysis of Organic Contaminants in Natural Environments: A Critical Review of the State of the Art, Prospects, and Future Challenges. *Anal. Bioanal. Chem.* **2004**, *378*, 283-300.

14. Ferrari, A. C.; Robertson, J. Interpretation of Raman Spectra of Disordered and Amorphous Carbon. *Phys. Rev. B* **2000**, *61*, 14095-14107.

15. Dresselhaus, M. S.; Dresselhaus, G.; Saito, R.; Jorio, A. Raman Spectroscopy of Carbon Nanotubes. **2005**, *409*, 47-99.

16. Ferrari, A. C., et al. Raman Spectrum of Graphene and Graphene Layers. *Phys. Rev. Lett.* **2006**, *97*, 187401.

17. Fan, F.; Feng, Z.; Li, C. Uv Raman Spectroscopic Studies on Active Sites and Synthesis Mechanisms of Transition Metal-Containing Microporous and Mesoporous Materials. *Accounts Chem. Res.* **2010**, *43*, 378-387.

18. Li, C.; Stair, P. C. Ultraviolet Raman Spectroscopy Characterization of Coke Formation in Zeolites. *Catal. Today* **1997**, *33*, 353-360.

19. Chua, Y. T.; Stair, P. C. A Novel Fluidized Bed Technique for Measuring Uv Raman Spectra of Catalysts and Adsorbates. *J. Catal.* **2000**, *196*, 66-72.

20. Chua, Y. T.; Stair, P. C. An Ultraviolet Raman Spectroscopic Study of Coke Formation in Methanol to Hydrocarbons Conversion over Zeolite H-Mfi. *J. Catal.* **2003**, *213*, 39-46.

21. Allotta, P. M.; Stair, P. C. Time-Resolved Studies of Ethylene and Propylene Reactions in Zeolite H-Mfi by in-Situ Fast Ir Heating and Uv Raman Spectroscopy. *ACS Catal.* **2012**, *2*, 2424-2432.

22. Beato, P.; Schachtl, E.; Barbera, K.; Bonino, F.; Bordiga, S. Operando Raman Spectroscopy Applying Novel Fluidized Bed Micro-Reactor Technology. *Catal. Today* **2013**, *205*, 128-133.

23. Ferguson, J.; Reeves, L. W.; Schneider, W. G. Vapor Absorption Spectra and Oscillator Strengths of Naphthalene, Anthracene, and Pyrene. *Can. J. Chem.* **1957**, *35*, 1117-1136.

24. Catalan, J.; Carlos Del Valle, J. A Spectroscopic Rule from the Solvatochromism of Aromatic Solutes in Nonpolar Solvents. *J. Phys. Chem. B* **2014**, *118*, 5168-5176.

25. Borodina, E.; Meirer, F.; Lezcano-González, I.; Mokhtar, M.; Asiri, A. M.; Al-Thabaiti, S. A.; Basahel, S. N.; Ruiz-Martinez, J.; Weckhuysen, B. M. Influence of the Reaction Temperature on the Nature of the Active and Deactivating Species During Methanol to Olefins Conversion over H-Ssz-13. *ACS Catal.* **2015**, *5*, 992-1003.

26. Asher, S. A.; Johnson, C. R. Raman Spectroscopy of a Coal Liquid Shows That Fluorescence Interference Is Minimized with Ultraviolet Excitation. *Science* **1984**, *225*, 311-313.

27. Guth, J. L.; Kessler, H.; Wey, R., New Route to Pentasil-Type Zeolites Using a Non Alkaline Medium in the Presence of Fluoride Ions. In *Studies in Surface Science and Catalysis*, Murakami, Y.; Iijima, A.; Ward, J. W., Eds. Elsevier: 1986; Vol. 28, pp 121-128.

28. Castiglioni, C.; Tommasini, M.; Zerbi, G. Raman Spectroscopy of Polyconjugated Molecules and Materials: Confinement Effect in One and Two Dimensions. *Phil. Trans. R. Soc. Lond. A* **2004**, *362*, 2425–2459.

29. Avila Ferrer, F. J.; Barone, V.; Cappelli, C.; Santoro, F. Duschinsky, Herzberg−Teller, and Multiple Electronic Resonance Interferential Effects in Resonance Raman Spectra and Excitation Profiles. The Case of Pyrene. *J. Chem. Theory Comput.* **2013**, *9*, 3597-3611.

30. Patterson, J. W. The Ultraviolet Absorption Spectra of Coronene. *J. Am. Chem. Soc.* **1942**, *64*, 1485-1486.

31. Bjorgen, M.; Bonino, F.; Kolboe, S.; Lillerud, K. P.; Zecchina, A.; Bordiga, S. Spectroscopic Evidence for a Persistent Benzenium Cation in Zeolite H-Beta. *J. Am. Chem. Soc.* **2003**, *125*, 15863-15868.

32. Bjorgen, M.; Bonino, F.; Arstad, B.; Kolboe, S.; Lillerud, K. P.; Zecchina, A.; Bordiga, S. Persistent Methylbenzenium Ions in Protonated Zeolites: The Required Proton Affinity of the Guest Hydrocarbon. *ChemPhysChem* **2005**, *6*, 232-235.

33. Márquez, F.; Zicovich-Wilson, C. M.; Corma, A.; Palomares, E.; García, H. Naphthalene Included within All-Silica Zeolites: Influence of the Host on the Naphthalene Photophysics. *J. Phys. Chem. B* **2001**, *105*, 9973-9979.

Table of Contents Graphic

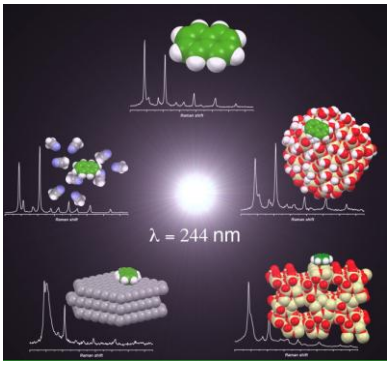

Supporting Information for:

In situ Resonant UV-Raman Spectroscopy of Polycyclic Aromatic Hydrocarbons

Matteo Signorile, Francesca Bonino, Alessandro Damin, and Silvia Bordiga*

Department of Chemistry, NIS and INSTM Reference Centre, University of Turin, Via G. Quarello 15, I-10135 and Via P. Giuria 7, I-10125, Turin, Italy

* Francesca Bonino, tel. +390116708383, fax. +390116707855, e-mail francesca.bonino@unito.it

Supplementary Information

Figure S1 UV Raman spectra of naphtalene collected preventing/not preventing photodecomposition.

Figure S2 Adsorption spectra of 10^{-5} M solution in acetonitrile of molecules.

Figure S3 Raman spectra of 0.1 M solution in acetonitrile of naphthalene collected with different excitation laser lines.

Figure S4 UV Raman spectrum of 0.1 M solution of benzene in acetonitrile in the 3100-300 cm^{-1} frequency range.

Figure S5 Background subtracted UV Raman spectra of molecules adsorbed from vapor phase on activated carbon.

Figure S1 shows an example of photoinduced degradation due to the excitation laser photons carrying very high energy (λ = 244 nm). The use of a specifically designed home-made sample holder avoids the degradation.

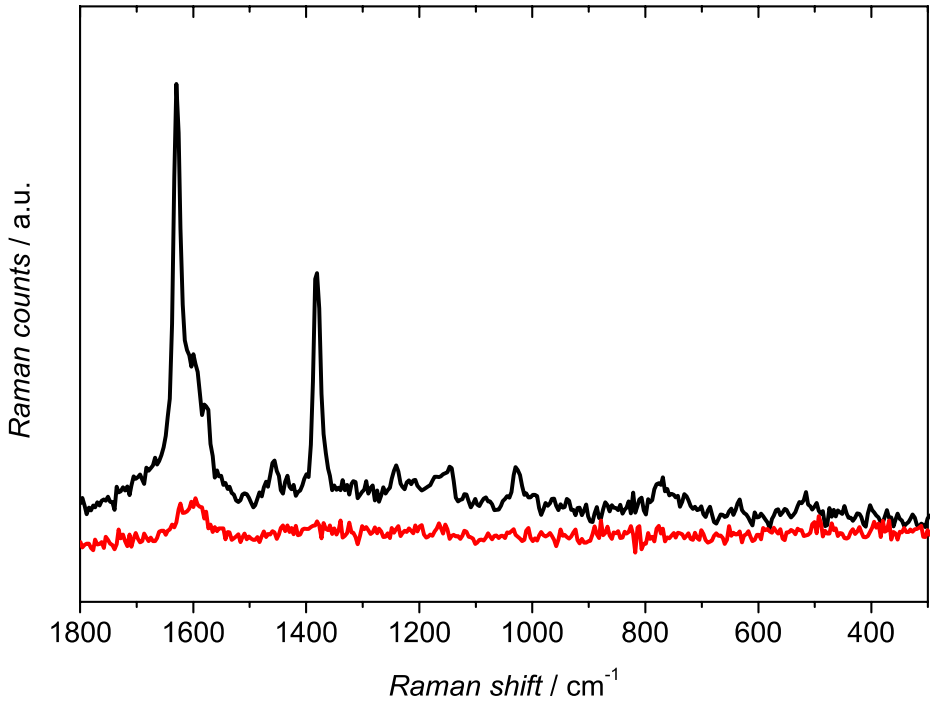

Figure S1. UV (λ = 244nm) Raman spectra of naphthalene, collected preventing the sample decomposition thanks to a specific home-made sample holder (solid black line) and without any precaution (solid red line). In this second case, the sample undergoes photodecomposition as testified by the complete transformation of its Raman spectrum.

Figure S2 shows the absorption spectra of the 10^{-5} M solutions of PAHs in CAN, measured in transmission on a Varian Cary300 spectrometer in the 200-800 nm range. The vertical bar shows the frequency of the UV laser used for excitation in the UV-Raman measurements: it is possible

to observe that most of the analyzed molecules present an electronic transition falling close to the laser frequency, allowing to achieve the resonance conditions.

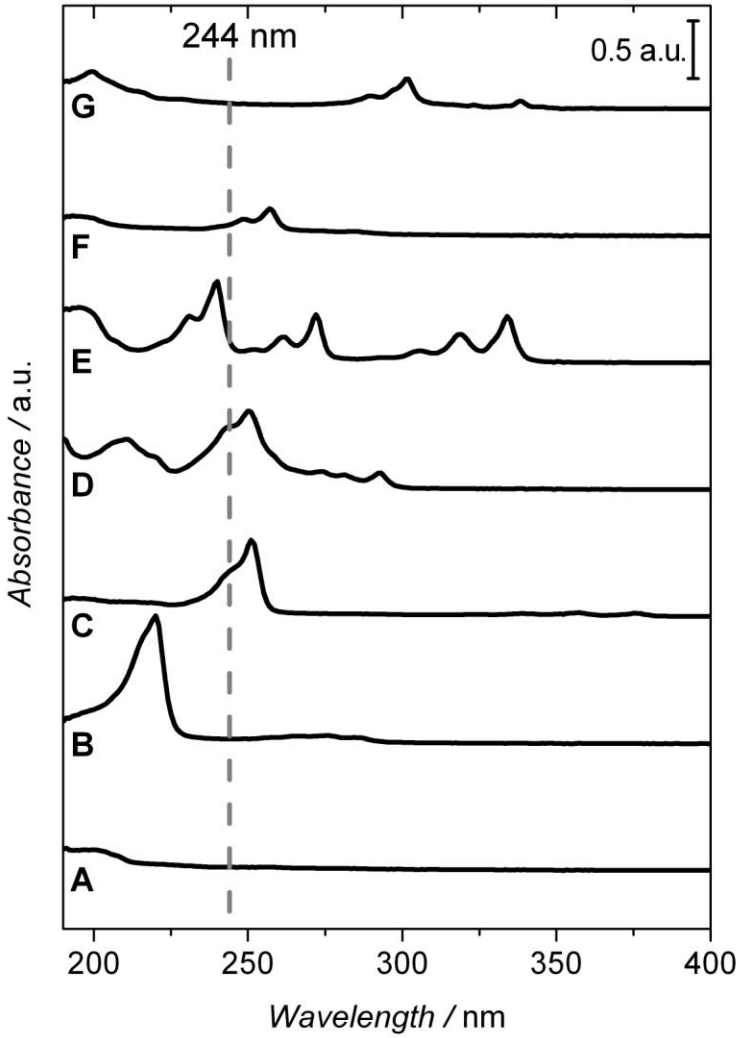

Figure S2. Absorption spectra of 10^{-5} M solutions in ACN of benzene **A**, naphthalene **B**, anthracene **C**, phenanthrene **D**, pyrene **E**, triphenylene **F** and coronene **G**. Spectra have been vertically shifted for a better comparison.

Figure S3 shows the Raman spectra of the 0.1 M solution of naphthalene in acetonitrile collected both with visible (λ = 785 nm and λ = 514 nm) and UV (λ = 244 nm) laser lines. The spectra collected with the visible excitation lines show very weak signals ascribable to naphthalene and most intense modes are related to the solvent. Conversely the sample vibrations are selectively enhanced by the resonant Raman effect when the spectrum is collected with the UV excitation source. In this way naphthalene can be detected, even if diluted, without relevant interferences from the solvent.

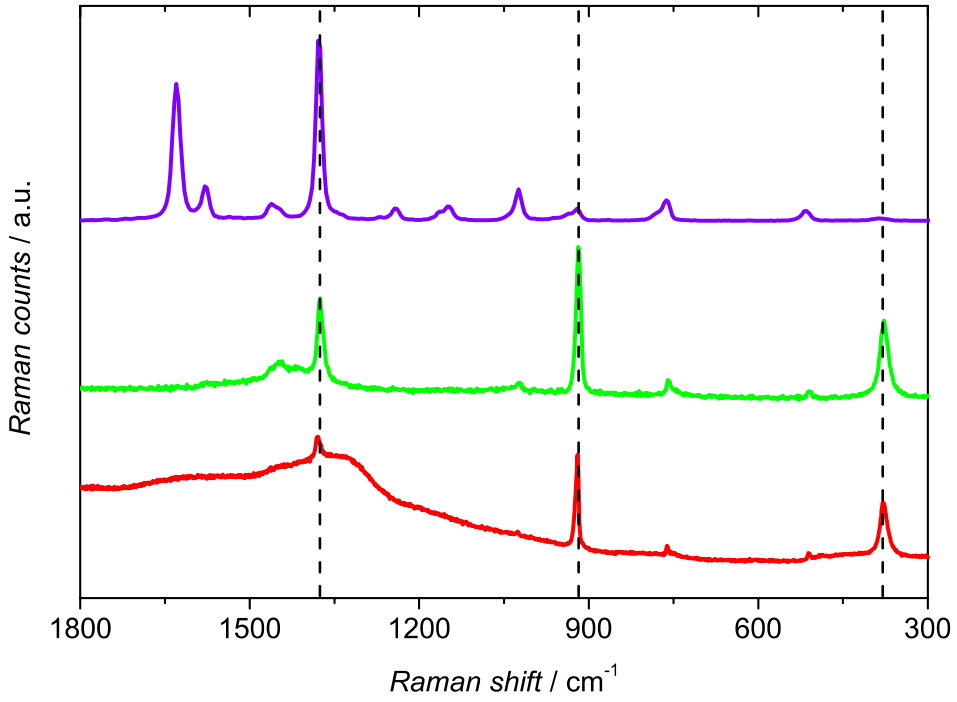

Figure S3. Raman spectra of 0.1M solution in acetonitrile of naphthalene, collected with different excitation laser lines: λ = 785 nm (solid red line); λ = 514 nm (solid green line); and λ = 244nm (solid violet line). The vertical dashed lines label the vibrational modes of the acetonitrile. Spectra have been rescaled and shifted for a better comparison.

The UV Raman spectrum of the 0.1M solution of benzene in acetonitrile is reported in an extended frequency range (3100-300 cm^{-1}) in Figure S4. The pronounced slope of the background in the high wavenumber region is due to the benzene emission (i.e. fluorescence) competing with the Raman signal of both acetonitrile and benzene itself. Moreover benzene absorbs most of the incident light, as the excitation wavelength (λ = 244 nm) matches with an electronic transition of the molecule. This results in an overall poor quality of the spectrum, where no signal related to the benzene can be identified.

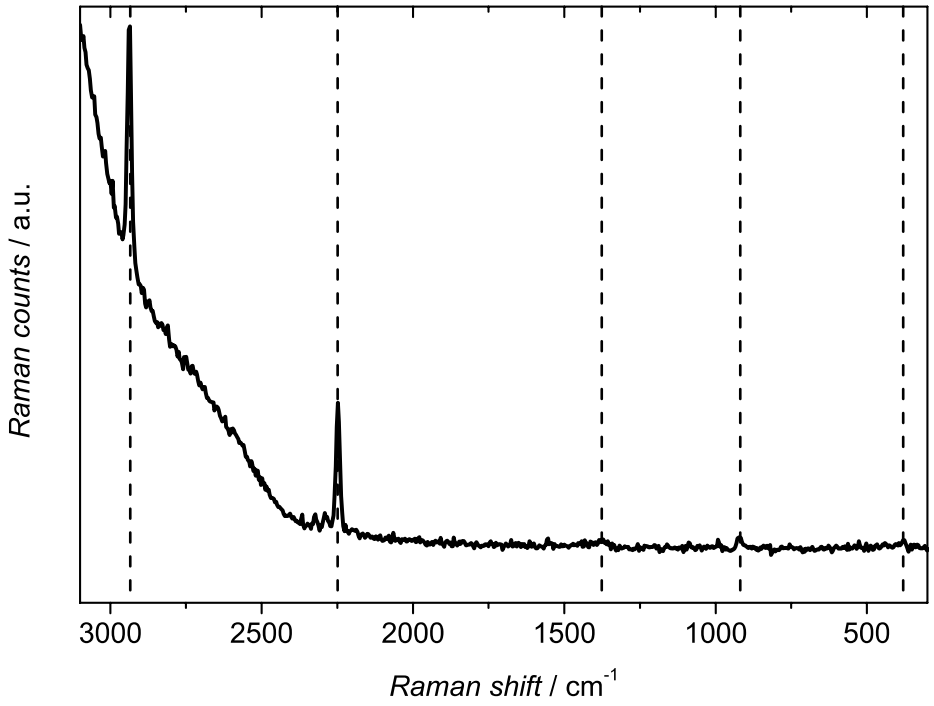

Figure S4. UV (λ = 244nm) Raman spectra of 0.1M solution of benzene. The vertical dashed lines label the vibrational modes of the acetonitrile.

The UV Raman spectra of PAHs adsorbed on activated carbon suffer the interference of the G band of carbon itself around 1600 cm^{-1}. In order to try to extract the information related to the molecules even from this region, the spectrum of the bare activated carbon has been subtracted

from the ones of PAHs adsorbed on it. The results are reported in Figure S5. The subtraction procedure allowed to better discriminate the vibrational modes of PAHs around the carbon G band, although the heavy noise makes the obtained spectra not fully reliable in terms of relative intensities.

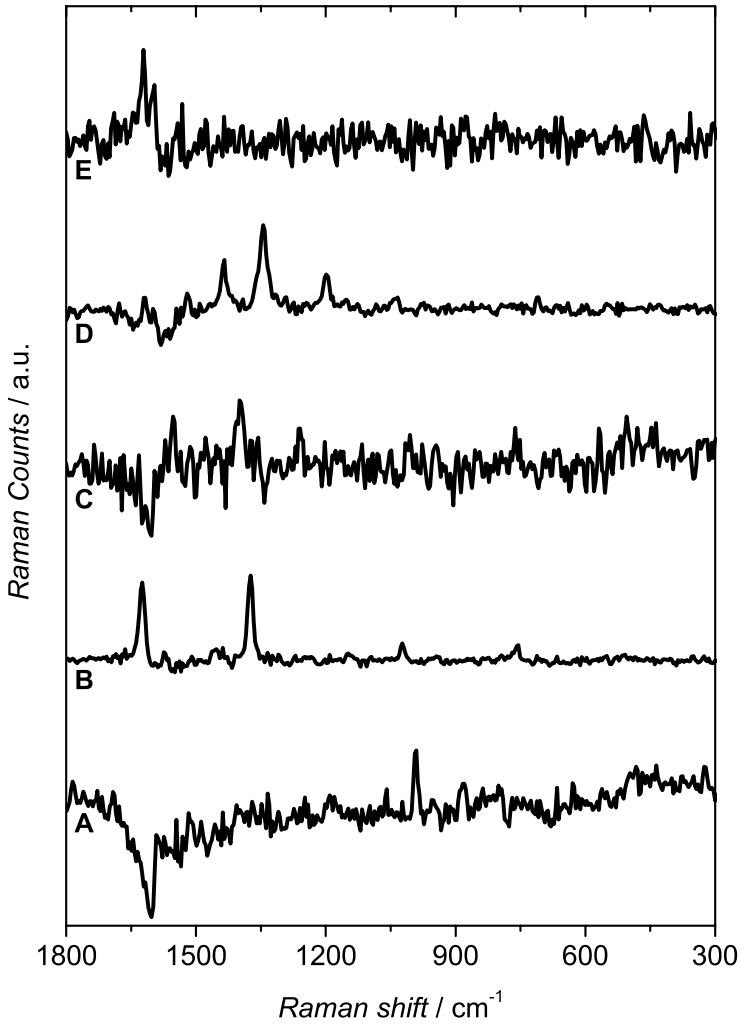

Figure S5. Background subtracted UV (λ = 244nm) Raman spectra of benzene **A**, naphthalene **B**, anthracene **C**, phenanthrene **D** and pyrene **E** adsorbed from vapor phase on activated carbon. Spectra have been rescaled and shifted for a better comparison.

Extendend references

7. Sandford, S. A.; Aleon, J.; Alexander, C. M. O.; Araki, T.; Bajt, S.; Baratta, G. A.; Borg, J.; Bradley, J. P.; Brownlee, D. E.; Brucato, J. R.; Burchell, M. J.; Busemann, H.; Butterworth, A.; Clemett, S. J.; Cody, G.; Colangeli, L.; Cooper, G.; D'Hendecourt, L.; Djouadi, Z.; Dworkin, J. P.; Ferrini, G.; Fleckenstein, H.; Flynn, G. J.; Franchi, I. A.; Fries, M.; Gilles, M. K.; Glavin, D. P.; Gounelle, M.; Grossemy, F.; Jacobsen, C.; Keller, L. P.; Kilcoyne, A. L. D.; Leitner, J.; Matrajt, G.; Meibom, A.; Mennella, V.; Mostefaoui, S.; Nittler, L. R.; Palumbo, M. E.; Papanastassiou, D. A.; Robert, F.; Rotundi, A.; Snead, C. J.; Spencer, M. K.; Stadermann, F. J.; Steele, A.; Stephan, T.; Tsou, P.; Tyliszczak, T.; Westphal, A. J.; Wirick, S.; Wopenka, B.; Yabuta, H.; Zare, R. N.; Zolensky, M. E., Organics Captured from Comet 81p/Wild 2 by the Stardust Spacecraft. *Science* **2006**, 314, 1720-1724.

16. Ferrari, A. C.; Meyer, J. C.; Scardaci, V.; Casiraghi, C.; Lazzeri, M.; Mauri, F.; Piscanec, S.; Jiang, D.; Novoselov, K. S.; Roth, S.; Geim, A. K., Raman Spectrum of Graphene and Graphene Layers *Phys. Rev. Lett.* **2006**, 97, 187401.